

**HETEROGENEOUS FENTON DEGRADATION
OF OFLOXACIN IN AQUEOUS SOLUTION
USING Fe_3O_4 -ZEOLITE,
 Fe_3O_4 -MONTMORILLONITE AND
 Fe_3O_4 -MONTMORILLONITE ALGINATE
COMPOSITES**

ALAMRI RAHMAH DHAHAWI

UNIVERSITI SAINS MALAYSIA

2023

**HETEROGENEOUS FENTON DEGRADATION
OF OFLOXACIN IN AQUEOUS SOLUTION
USING Fe_3O_4 -ZEOLITE,
 Fe_3O_4 -MONTMORILLONITE AND
 Fe_3O_4 -MONTMORILLONITE ALGINATE
COMPOSITES**

by

ALAMRI RAHMAH DHAHAWI

**Thesis submitted in fulfilment of the requirements
for the degree of
Doctor of Philosophy**

April 2023

ACKNOWLEDGEMENT

I would like to thank Allah Almighty once again for giving me the strength, knowledge, ability and opportunity to undertake this research study and to persevere and complete it satisfactorily. Without His blessings, this achievement would not have been possible. Peace and blessings of Allah are upon our noble prophet Muhammad peace be upon him, his companions and who so ever followed their footsteps till the day of resurrection.

It is time to express my thanks and gratitude to my dear supervisor, Professor Dr. Rohana Adnan, for her continuous support, advice, encouragement, suggestions by providing me with information and her complete confidence in me that made me able to do the right things in the right way. I am very fortunate to have a wonderful supervisor in giving me directions which has had significant impact in the completion of this thesis. May Allah protect her and bless her.

I would like to express my thanks to my co- supervisor, Dr. Oh Wen Da, for his quick responses to my questions throughout my research work. I would also like to thank my lab members; Dr. Saifullahi, Atilia, Anis, Dr. Sadiq, Promise, and Nazz for for their unlimited and unconditional support. May Allah bless them all.

Finally, I would like to share my appreciation and gratitude to both of my parents, my lovely husband Ali and my children (Murad and Mira) and the rest of my brothers, sisters and friends for their continuous love, patience, encouragement and prayers given during the period of completing this thesis.

TABLE OF CONTENTS

ACKNOWLEDGEMENT	ii
TABLE OF CONTENTS	iii
LIST OF TABLES	ix
LIST OF FIGURES	xi
LIST OF ABBREVIATIONS	xvii
LIST OF APPENDICES	xix
ABSTRAK	xx
ABSTRACT	xxii
CHAPTER 1 INTRODUCTION	1
1.1 Background	1
1.2 Problem Statements.....	3
1.3 Objectives of the Proposed Study	6
1.4 Scope of Study	7
1.5 Hypothesis and Significance of the Study	7
1.6 Thesis Outline	8
CHAPTER 2 LITERATURE REVIEW	9
2.1 Background	9
2.2 Ofloxacin.....	10
2.3 Wastewater Treatment Methods	13
2.3.1 Fenton Process	17
2.4 Magnetite, Fe ₃ O ₄	26
2.5 Zeolite	27
2.6 Clay and Clay like Materials.....	29
2.6.1 Montmorillonite	31
2.7 Biopolymer and its application in wastewater treatment.....	32

2.7.1	Sodium Alginate (SA).....	39
CHAPTER 3 MATERIALS AND METHODS		41
3.1	Materials.....	41
3.2	Synthesis of Fe ₃ O ₄ -Zeolite and Fe ₃ O ₄ -Clay Based Composites.....	42
3.2.1	Synthesis of Fe ₃ O ₄ -Zeolite (FeZ) Composites.....	42
3.2.2	Synthesis of Fe ₃ O ₄ -Montmorillonite (FeM) Composites.....	43
3.2.3	Synthesis of FeM-10/Alginate Beads	43
3.3	Characterizations.....	44
3.3.1	X-Ray Photoelectron Spectroscopy	44
3.3.2	Scanning Electron Microscopy and Energy Dispersive X-Ray	44
3.3.3	Transmission Electron Microscopy	45
3.3.4	Fourier Transform Infrared Spectroscopy.....	45
3.3.5	N ₂ Adsorption - Desorption	46
3.3.6	Thermogravimetric Analysis.....	46
3.3.7	Determination of pH of Point of Zero Charge (pH _{PZC}).....	47
3.3.8	UV-Visible Spectroscopy	47
3.3.9	Total Organic Carbon (TOC).....	47
3.3.10	Atomic Absorption Spectroscopy (AAS)	48
3.3.11	Leaching Test.....	49
3.4	Fenton Degradation of OFL using Fe ₃ O ₄ -Zeolite and Fe ₃ O ₄ -Clay Based Composites	49
3.4.1	Fenton Degradation of OFL using Fe ₃ O ₄ -Zeolite (FeZ) Composites.....	49
3.4.2	Fenton Degradation of OFL using Fe ₃ O ₄ -Montmorillonite (FeM) Composites.....	51
3.4.3	Fenton Degradation of OFL using FeM-10/Alginate Beads.....	51
3.5	Reusability Studies.....	52

CHAPTER 4 RESULTS AND DISCUSSION

CHARACTERIZATIONS AND FENTON CATALYTIC ACTIVITY OF Fe₃O₄-ZEOLITE (FeZ) COMPOSITES 53

4.1	Characterizations of Fe ₃ O ₄ -Zeolite Composites	53
4.1.1	X-ray Photoelectron Spectroscopy (XPS).....	53
4.1.2	Field Emission Scanning Electron Microscope (FESEM) Analysis.....	58
4.1.3	Transmission Electron Microscope (TEM).....	60
4.1.4	Fourier Transform Infra-red (FTIR) Spectroscopy	62
4.1.5	pH of Point of Zero Charge (pH _{PZC})	63
4.1.6	Nitrogen Adsorption-Desorption Analysis	64
4.2	Catalytic Study of Fe ₃ O ₃ -Zeolite Composites	67
4.2.1	OFL Removal in Different Processes	67
4.2.2	Effect of Fe ₃ O ₄ Loadings on Zeolite.....	68
4.2.3	Effect of Catalyst Dosage	70
4.2.4	Effect of Initial Solution pH.....	71
4.2.5	Effect of Initial OFL Concentration.....	72
4.2.6	Effect of Different Oxidants	73
4.2.6(a)	Kinetic Studies on the Effect of Different Oxidants	74
4.2.7	Effect of H ₂ O ₂ Dosage	75
4.2.8	Effect of Reaction Temperature.....	76
4.2.8(a)	Kinetic Studies on the Effect of Reaction Temperature	77
4.2.9	Effect of Inorganic Salts	80
4.2.10	Total Organic Carbon TOC Removal Studies	81
4.2.11	Leaching Studies in Various Leachants	82
4.2.12	Hetero-Fenton Degradation Mechanism.....	83
4.2.13	Reusability, Leaching and Stability Studies	84

CHAPTER 5 RESULTS AND DISCUSSION

CHARACTERIZATIONS AND CATALYTIC STUDY OF Fe₃O₄-MONTMORILLONITE COMPOSITES..... 87

5.1	Characterizations of Fe ₃ O ₄ -Montmorillonite Composites	87
5.1.1	X-ray Photoelectron Spectroscopy (XPS).....	87
5.1.2	Field Emission Scanning Electron Microscope (FESEM) Analysis.....	92
5.1.3	Transmission electron microscope (TEM).....	94
5.1.4	Fourier Transform Infra-red (FTIR) Spectroscopy	96
5.1.5	Nitrogen Adsorption-Desorption Analysis	97
5.1.6	pH of Point of Zero Charge (pH _{PZC})	99
5.2	Catalytic Study Using Fe ₃ O ₄ -Montmorillonite Composites	100
5.2.1	Removal of OFL via Different Processes	100
5.2.2	Effect of Fe ₃ O ₄ Loadings on the OFL Degradation via Fenton Process	102
5.2.3	Effect of Catalyst Dosage	103
5.2.4	Effect of Initial Solution pH.....	104
5.2.5	Effect of Initial OFL Concentration.....	106
5.2.6	Effect of Different Oxidants	107
5.2.6(a)	Kinetic Studies on the Effect of Different Oxidants	107
5.2.7	Effect of H ₂ O ₂ Dosage	109
5.2.8	Effect of Reaction Temperature	109
5.2.8(a)	Kinetic Studies on the Effect of Reaction Temperature	110
5.2.9	Effect of Inorganic Salts	113
5.2.10	Total Organic Carbon (TOC) Removal Studies.....	115
5.2.11	Leaching Studies in Various Leachants	115
5.2.12	Hetero-Fenton Degradation Mechanism.....	116

5.2.13	Reusability, Leaching and Stability Studies	117
--------	---	-----

CHAPTER 6 RESULTS AND DISCUSSION

	CHARACTERIZATIONS AND FENTON CATALYTIC ACTIVITY OF Fe₃O₄-MONTMORILLONITE-ALGINATE (FeMA) COMPOSITE BEADS.....	120
6.1	Introduction.....	120
6.2	Characterizations of Pristine Alginate and Fe ₃ O ₄ -Montmorillonite-Alginate.....	121
6.2.1	Physical Observations of the Fe ₃ O ₄ -Montmorillonite-Alginate	121
6.2.2	X-ray Photoelectron Spectroscopy (XPS).....	123
6.2.3	Field Emission Scanning Electron Microscope (FESEM) Analysis.....	127
6.2.4	Fourier Transform Infra-red (FTIR) Spectroscopy	129
6.2.5	Nitrogen Adsorption-Desorption Analysis	131
6.2.6	Thermogravimetric Analysis (TGA).....	133
6.2.7	pH of Point of Zero Charge (pH _{PZC})	134
6.3	OFL Removal Study Using Fe ₃ O ₄ -Montmorillonite-Alginate Composite Beads.....	135
6.3.1	OFL Removal in Different Processes	135
6.3.2	Effect of Fe ₃ O ₄ -Montmorillonite Loading on Alginate	137
6.3.3	Effect of Fe ₃ O ₄ -Montmorillonite-Alginate Composite Beads Dosage.....	138
6.3.4	Effect of Initial Solution pH.....	139
6.3.5	Effect of Initial OFL Concentration.....	140
6.3.6	Effect of Different Oxidants	141
6.3.7	Effect of H ₂ O ₂ Dosage	143
6.3.8	Effect of Reaction Temperature.....	144
6.3.8(a)	Kinetic Studies of the Effect of Reaction Temperature on Fenton Degradation Efficiency of OFL	145

6.3.9	Effect of Inorganic Salts	147
6.3.10	Total Organic Carbon (TOC) Removal Studies.....	147
6.3.11	Photo-Fenton Catalytic Activity	148
6.3.12	Leaching Studies in Various Leachants	150
6.3.13	Proposed Mechanism for Hetero-Fenton Degradation Using FeMA Composite Beads	150
6.3.14	Reusability, Leaching and Stability Studies	151
6.3.15	Comparison of the Performance of FeZ-8, FeM-10 and FeMA-2.....	154
CHAPTER 7 CONCLUSIONS AND RECOMMENDATIONS.....		155
7.1	Conclusions.....	155
7.2	Recommendations for Future Studies	157
REFERENCES.....		158
APPENDICES		
LIST OF PUBLICATIONS AND PRESENTATIONS		

LIST OF TABLES

	Page
Table 2.1	Molecular structure and some physicochemical properties of OFL..... 11
Table 2.2	Different wastewater treatment methods and their advantages and limitations..... 14
Table 2.3	Efficiencies during the treatment of OFL polluted water via Fenton process. 22
Table 2.4	Summary of the literature on the use of biopolymers in Fenton oxidation process for the treatment of organic/inorganic pollutants in water. 35
Table 3.1	List of chemicals used in the present study, their purity and brand. 41
Table 4.1	Elemental composition of zeolite and FeZ composites as determined by EDX 60
Table 4.2	Surface area and pore volume of bare zeolite and FeZ composites. 65
Table 4.3	Parameters of linear regression for different kinetic models for the Fenton degradation of OFL using different oxidants..... 75
Table 4.4	Parameters of linear regression for different kinetic models for the Fenton degradation of OFL at different reaction temperatures..... 79
Table 5.1	Elemental composition of montmorillonite and FeM composites as determined by EDX..... 94
Table 5.2	Surface area and pore volume of bare montmorillonite and FeM composites..... 99
Table 5.3	Parameters of linear regression for different kinetic models for the Fenton degradation of OFL using different oxidants..... 108
Table 5.4	Parameters of linear regression for different kinetic models for the Fenton degradation of OFL using FeM-10 at different reaction temperatures..... 111
Table 5.5	Activation energies for the heterogeneous Fenton degradation of some pollutants..... 113

Table 6.1	Diameters of wet and dried bare alginate and FeMA composite beads.....	123
Table 6.2	Composition of bare alginate and FeMA composite beads as determined by EDX.	129
Table 6.3	Surface area and pore volume of bare alginate and FeMA composite beads.....	132
Table 6.4	Parameters of linear regression for different kinetic models for the degradation of OFL using different oxidants.	142
Table 6.5	Parameters of linear regression for different kinetic models for the degradation of OFL at different temperatures.....	146

LIST OF FIGURES

	Page
Figure 1.1	Sources of water pollution..... 1
Figure 1.2	Pathways of antibiotics in different environmental matrices (Bhagat et al., 2020). 4
Figure 2.1	Contaminants of emerging concern and existing challenges in their treatment (Reddy, 2017)..... 9
Figure 2.2	Summary of the different advanced oxidation processes (Gautam et al., 2019). 16
Figure 2.3	Heterogeneous Fenton degradation (Rusevova et al., 2012). 17
Figure 2.4	Classification of Fenton process (Nidheesh et al., 2013). 18
Figure 2.5	The inverse spinel structure of magnetite Fe ₃ O ₄ (Rivani et al., 2019). 26
Figure 2.6	Zeolite mineral molecular structure (Vimonses et al., 2009). 27
Figure 2.7	Schematic drawing of the structure of typical synthetic zeolites: (a) A-types, (b) faujasites, (c) ZSM-5 and (d) ZK-5 (Kalogeras and Vassilikou-Dova, 1998). 28
Figure 2.8	2D layered zeolite precursor (e.g., PREFER (precursor of ferrierite) as an example) with highlights of the -OH group, d(OH...OH), Q ³ and Q ⁴ coordination structures, and the definition of member ring (MR) in zeolites. Both line (a) and ball-stick (b) display styles are included. (c) shows the Q ³ and Q ⁴ structures in zeolites or their precursors (Schulman et al., 2020). 29
Figure 2.9	Schematic representation of the basic structure of a clay mineral, with tetrahedral and octahedral arrangements of atoms in sheets, separated by cations and water in the interlayer between the silicate sheets (Williams & Haydel, 2010). 30
Figure 2.10	Schematic representation of the structure of montmorillonite (a) Side view: tetrahedrons units of montmorillonite assembled through weak van der Waals and electrostatic forces to form the primary particles, (b) Top view of montmorillonite, hexagonal structure of oxygen and hydroxyl ligands of the octahedral layer (Zhou et al., 2019). 31

Figure 2.11	Overview of different biopolymers including synthetic (biodegradable) and naturally derived polymers (Strassburg et al., 2020).	33
Figure 2.12	Molecular structure of sodium alginate (Salisu et al., 2016).....	39
Figure 3.1	Summary of the research conducted in this work.....	42
Figure 4.1	XPS spectra of (a) zeolite, (b) FeZ-1.5, (c) FeZ-3, (d) FeZ-5, (e) FeZ-8 and (f) FeZ-10.	54
Figure 4.2	Deconvoluted XPS spectra of (a) Si 2p, (b) O 1s for zeolite, and (c) Si 2p, (d) O 1s for FeZ-8 composite.....	58
Figure 4.3	FESEM images of (a) zeolite, (b) FeZ-1.5, (c) FeZ-3, (d) FeZ-5, (e) FeZ-8 and (f) FeZ-10.....	59
Figure 4.4	TEM images of zeolite (a) zeolite, (b) FeZ-1.5, (c) FeZ-3, (d) FeZ-5, (e) FeZ-8 and (f) FeZ-10.....	61
Figure 4.5	FTIR spectra of bare zeolite and FeZ composites.	62
Figure 4.6	Point of zero charges of pristine zeolite and FeZ composites.	64
Figure 4.7	N ₂ adsorption – desorption isotherms and the corresponding pore size distribution (insets) for zeolite (a), FeZ-1.5 (b), FeZ-3 (c), FeZ-5 (d), FeZ-8 (e) and FeZ-10 (f) composites.....	66
Figure 4.8	Removal efficiencies of OFL in different processes.	67
Figure 4.9	Effect of Fe ₃ O ₄ loading on zeolite on the degradation of OFL using FeZ.	69
Figure 4.10	Effect of FeZ-8 dosage on the degradation of OFL using FeZ-8.	70
Figure 4.11	Effect of initial solution pH on the degradation of OFL using FeZ-8.	72
Figure 4.12	Effect of initial OFL concentration on the degradation efficiency using FeZ-8.....	73
Figure 4.13	Effect of different oxidants on the degradation efficiency of OFL using FeZ-8.	74
Figure 4.14	Plots of (a) ln(C ₀ /C) versus t based on pseudo-first-order kinetics model and (b) 1/C – 1/C ₀ versus t based on pseudo-second-order kinetics model for the effect of different oxidants on the degradation of OFL using FeZ-8.....	75

Figure 4.15	Effect of H ₂ O ₂ dosage on the degradation efficiency of OFL using FeZ-8.....	76
Figure 4.16	Effect of reaction temperature on the degradation efficiency of OFL using FeZ-8.....	77
Figure 4.17	(a) ln(C ₀ /C) versus t plots based on pseudo-first-order kinetics model and (b) 1/C – 1/C ₀ versus t plots based on pseudo-second-order kinetics model for the effect of reaction temperature on the degradation of OFL using FeZ-8.....	78
Figure 4.18	Plot of ln k against 1/T for the Fenton degradation of OFL using FeZ-8 catalyst.....	79
Figure 4.19	Effect of inorganic salts on the degradation efficiency of OFL using FeZ-8.	80
Figure 4.20	Comparison of the TOC removal efficiency using FeZ-8.	82
Figure 4.21	Effect of leaching agents on iron leaching from FeZ-8 catalyst.	83
Figure 4.22	Proposed mechanism for OFL degradation using FeZ composite as hetero-Fenton catalyst.....	84
Figure 4.23	Recyclability of FeZ-8 catalyst for Fenton degradation of OFL.....	85
Figure 4.24	Effect of consecutive cycles on the leaching of Fe.....	85
Figure 4.25	FTIR spectra of FeZ-8 catalyst (a) fresh and (b) after five cycles.	86
Figure 5.1	XPS spectra of montmorillonite (a), FeM-3 (b), FeM-5 (c), FeM-8 (d), FeM-10 (e) and FeM-15 (f).....	88
Figure 5.2	Deconvoluted XPS spectra of (a) Si 2p, (b) O 1s for montmorillonite, and (c) Si 2p, (d) O 1s for FeM-10 composite.....	91
Figure 5.3	FESEM images of (a) montmorillonite, (b) FeM-3, (c) FeM-5, (d) FeM-8 (e) FeM-10, and (f) FeM-15.....	93
Figure 5.4	TEM images of (a) montmorillonite, (b) FeM-3, (c) FeM-5, (d) FeM-8, (e) FeM-10, and (f) FeM-15.....	95
Figure 5.5	FTIR spectra of bare montmorillonite and FeM composites.....	96
Figure 5.6	N ₂ adsorption – desorption isotherms and the corresponding pore size distribution (insets) for montmorillonite (a), FeM-3 (b), FeM-5 (c), FeM-8 (d), FeM-10 (e) and FeM-15 (f) composites.	98

Figure 5.7	Point of zero charges (pH_{PZC}) of pristine montmorillonite and FeM composites.....	99
Figure 5.8	The graph showing the percentage of OFL removal in different processes.	100
Figure 5.9	Effect of Fe_3O_4 loadings on montmorillonite in the Fenton oxidation of OFL using FeM composites.....	103
Figure 5.10	Effect of Fe_3O_4 loading on montmorillonite in the Fenton oxidation of OFL using FeM-10.....	104
Figure 5.11	Effect of initial solution pH on the degradation of OFL using FeM-10.	105
Figure 5.12	Effect of initial OFL concentration on the degradation efficiency using FeM-10.....	106
Figure 5.13	Effect of different oxidants on the Fenton oxidation of OFL using FeM-10.....	107
Figure 5.14	(a) $\ln(C_0/C)$ versus t plots based on pseudo-first-order kinetics model and (b) $1/C - 1/C_0$ versus t plots based on pseudo-second-order kinetics model for the effect of different oxidants on the degradation of OFL using FeM-10.	108
Figure 5.15	Effect of H_2O_2 dosage on Fenton oxidation of OFL using FeM-10.	109
Figure 5.16	Effect of reaction temperature on Fenton oxidation of OFL using FeM-10.....	110
Figure 5.17	(a) $\ln(C_0/C)$ versus t plots based on pseudo-first-order kinetics model and (b) $1/C - 1/C_0$ versus t plots based on pseudo-second-order kinetics model for the effect of temperature on the degradation of OFL using FeM-10.....	111
Figure 5.18	Plot of $\ln k$ against $1/T$ for the Fenton degradation of OFL using FeM-10 catalyst.	112
Figure 5.19	Effect of inorganic salts on the degradation efficiency of OFL using FeM-10.	114
Figure 5.20	TOC removal using FeM-10.....	115
Figure 5.21	Effect of leaching agents on iron leaching from FeM-10 catalyst.	116
Figure 5.22	Proposed mechanism for OFL degradation using FeM composite as a hetero-Fenton catalyst.	117

Figure 5.23	Recyclability of FeM-10 catalyst for Fenton degradation of OFL.....	117
Figure 5.24	Effect of consecutive cycles on the leaching of Fe.....	118
Figure 5.25	FTIR spectra of (a) fresh FeM-10 catalyst and (b) after fifth cycles.	119
Figure 6.1	Schematic representation of the calcium-induced gelation of alginate in accordance with the “egg-box” structure (Christensen et al., 1990).....	121
Figure 6.2	Photos of wet beads of (a) pristine alginate, (b) FeMA-0.5, (c) FeMA-1, (d) FeMA-2 and (e) FeMA-3.....	122
Figure 6.3	Photos of dry beads of (a) pristine alginate, (b) FeMA-0.5, (c) FeMA-1, (d) FeMA-2 and (e) FeMA-3.....	123
Figure 6.4	XPS spectra of pristine alginate (a), FeMA-0.5 (b), FeMA-1 (c), FeMA-2 (d) and FeMA-3 (e) composite beads.....	124
Figure 6.5	Deconvoluted Fe 2p XPS spectra of (a) FeM-10 and (b) FeMA-2 composite bead.	127
Figure 6.6	FESEM images of pristine alginate (a), FeMA-0.5 (b), FeMA-1 (c), FeMA-2 (d) and FeMA-3 (e) composite beads.....	128
Figure 6.7	FTIR spectra of pristine alginate and FeMA composite beads.	130
Figure 6.8	N ₂ adsorption – desorption isotherms and the corresponding pore size distribution (insets) of pristine alginate (a), FeMA-0.5 (b), FeMA-1 (c), FeMA-2 (d) and FeMA-3 (e) composite beads.....	131
Figure 6.9	TGA curves of pristine alginate and FeMA composite beads.	134
Figure 6.10	Point of zero charges of pristine alginate and FeMA composites.	135
Figure 6.11	The graph showing the OFL removal in different processes.....	136
Figure 6.12	Effect of Fe ₃ O ₄ -montmorillonite loading on alginate beads on the removal efficiency.	137
Figure 6.13	Effect of FeMA-2 dosage on the degradation of OFL.....	138
Figure 6.14	Effect of initial solution pH on the Fenton degradation of OFL using FeMA-2 composite beads.....	139

Figure 6.15	Effect of initial OFL concentration on the Fenton oxidation process using FeMA-2 composite beads.	140
Figure 6.16	Effect of different oxidants on the degradation efficiency of OFL using FeMA-2 beads.	141
Figure 6.17	(a) $\ln(C_0/C)$ versus t plots based on pseudo-first-order kinetics model and (b) $1/C - 1/C_0$ versus t plots based on pseudo-second-order kinetics model for the effect of different oxidants on the degradation of OFL using FeMA-2 beads	142
Figure 6.18	Effect of H_2O_2 dosage on the degradation efficiency of OFL using FeMA-2 beads.....	143
Figure 6.19	Effect of reaction temperature on the degradation efficiency of OFL using FeMA-2 beads.....	144
Figure 6.20	(a) $\ln(C_0/C)$ versus t plots based on pseudo-first-order kinetics model and (b) $1/C - 1/C_0$ versus t plots based on pseudo-second-order kinetics model for the effect of different reaction temperatures on the degradation of OFL using FeMA-2 beads.....	145
Figure 6.21	Plot of $\ln k$ against $1/T$ for the Fenton degradation of OFL using FeMA-2 composite beads.	146
Figure 6.22	Effect of inorganic salts on the degradation efficiency of OFL using FeMA-2 beads	147
Figure 6.23	TOC removal using FeMA-2 composite beads.	148
Figure 6.24	Degradation of OFL under different conditions.....	149
Figure 6.25	Effect of leaching agents on iron leaching from FeMA-2 catalyst.....	150
Figure 6.26	Proposed mechanism for the activation of H_2O_2 by FeMA composite beads via heterogenous Fenton process	151
Figure 6.27	Recycled FeMA-2 composite beads for Fenton degradation of OFL.	152
Figure 6.28	Effect of consecutive cycles on the leaching of Fe.....	153
Figure 6.29	FTIR spectra of FeMA-2 composite beads (a) fresh and (b) after fifth cycles of Fenton oxidation process.	153

LIST OF ABBREVIATIONS

•OH	Hydroxyl Radical
A	Absorbance
AOPs	Advanced Oxidation Processes
ATR	Attenuated Total Reflectance
BET	Brunauer – Emmet – Teller
BJH	Barret – Joyner – Halenda
Dis	Dispersed
E%	Percent Efficiency
ECs	Emerging Contaminants
eV	Photon Energy
FCC	Face Centered Cubic
Fe ₃ O ₄	Iron Oxide
FeM	Fe ₃ O ₄ -Montmorillonite
FeMA	Fe ₃ O ₄ -Montmorillonite-Alignate
FESEM	Field Emission Scanning Electron Microscopy
FeZ	Fe ₃ O ₄ -Zeolite
FTIR	Fourier Transform Infra-Red
IUPAC	International Union of Pure and Applied Chemistry
k ₁	Pseudo-first-order rate constant
k ₂	Pseudo-second-order rate constant
Min	Minutes
mL	Milliliter
MPSi	Mesoporous silica

NAA	Nitrogen Adsorption Analysis
OFL	Ofloxacin
PCPs	Personal Care Products
pH _{PZC}	pH of Point of Zero Charge
ppm	Parts Per Million
R ²	Correlation Coefficient
SBA-15	Santa Barbara Amorphous-15
Sep	Sepiolite
TEM	Transmission Electron Microscope
TGA	Thermogravimetric Analysis
TOC	Total Organic Carbon
wt%	Weight Percent
WWTP	Wastewater Treatment Plant
XPS	X-ray Photoelectron Spectroscopy

LIST OF APPENDICES

- Appendix A FESEM images of pristine alginate (a), FeMA-0.5 (b), FeMA-1 (c), FeMA-2 (d) and FeMA-3 (e) composite beads.
- Appendix B Measuring the diameter of pristine alginate (a), FeMA-0.5 (b), FeMA-1 (c), FeMA-2 (d) and FeMA-3 (e) composite beads.
- Appendix C Calibration curve for iron standard solution.

**DEGRADASI FENTON HETEROGEN OFLOXACIN DALAM LARUTAN
AKUEUS MENGGUNAKAN KOMPOSIT Fe₃O₄-ZEOLIT, Fe₃O₄-
MONTMORILLONIT DAN Fe₃O₄-MONTMORILLONIT ALGINAT**

ABSTRAK

Matlamat utama kajian ini adalah untuk membangunkan pemangkin heterogen yang menjimatkan, stabil dan berkesan untuk pemulihan air sisa melalui proses pengoksidaan Fenton. Fe₃O₄ diketahui boleh mengaktifkan H₂O₂ bagi menghasilkan radikal hidroksil dengan berkesan, bagaimanapun nanozarah yang terhasil mudah teraglomerat. Bagi mengatasi masalah ini, komposit Fe₃O₄ berasaskan zeolit (FeZ) dan tanah liat montmorilonit (FeM) telah disintesis melalui kaedah kopemendakan yang mudah dan dicirikan menggunakan pelbagai teknik. Prestasi setiap pemangkin telah dinilai melalui degradasi Fenton ofloksacin (OFL), sejenis antibiotik dan bahan pencemar tegar disebabkan oleh keaktifannya yang tinggi dan kebolehbiodegrasinya yang lemah. Kesan parameter seperti jumlah prekursor garam Fe, dos pemangkin, pH larutan awal, kepekatan awal OFL, isipadu H₂O₂, jenis agen pengoksidaan, suhu tindak balas dan garam bukan organik keatas peratus penyingkiran OFL telah dikaji. Pemuatan Fe₃O₄ ke atas zeolit menghasilkan komposit dengan luas permukaan dan isipadu liang yang lebih tinggi. Keputusan eksperimen mendedahkan bahawa sebanyak 88% OFL dan 51.2% jumlah karbon organik (TOC) boleh disingkirkan dari larutan akueus OFL 20 mg/L dalam tempoh 120 minit menggunakan pemangkin Fenton heterogen FeZ-8 pada keadaan optimum. Oleh kerana kemampuan montmorilonit menjerap ofloksacin lebih tinggi, kepekatan awal OFL telah diselaraskan dari 20 kepada 50 mg/L bagi komposit FeM. Seterusnya, kecekapan FeM dalam menyingkirkan OFL dari larutan akueus turut dikaji menggunakan parameter yang

sama. Pada keadaan optimum dan pH semula jadi OFL, peratus penyingkiran OFL melalui degradasi proses heterogen Fenton dengan kehadiran H_2O_2 adalah 81%, manakala jumlah pengurangan jumlah karbon organik (TOC) adalah kira-kira 56% dalam tempoh 120 minit. Kedua-dua komposit FeZ dan FeM menunjukkan penurunan peratus penyingkiran OFL sebanyak 8.89 dan 21.42% masing-masing pada kitaran ke 5 dan perkara ini dijangkakan adalah disebabkan oleh kadar larut resap larutan ion Fe yang tinggi iaitu 56.19 dan 65.37% masing-masing. Oleh kerana kecekapan degradasi Fenton FeM lebih tinggi berbanding FeZ, komposit FeM telah diimobilisasikan keatas kalsium alginat membentuk manik komposit FeMA bagi mengatasi masalah ini. Pada keadaan yang sama, peratus penyingkiran OFL oleh FeMA menghampiri 80% dan pengurangan TOC mencapai 53% dengan penurunan peratus penyingkiran yang minimal (2%) pada kitaran ke 5. Manik komposit FeMA boleh diasingkan dengan mudah, dikitar semula dan larut resap ion dari mangkin adalah rendah, 0.142 mg/L (pada kitaran ke 5). Berdasarkan keputusan eksperimen, dapat disimpulkan bahawa komposit berasaskan tanah liat FeMA yang disintesis berpotensi besar sebagai pemangkin heterogen Fenton untuk digunakan bagi degradasi bahan pencemar organik seperti antibiotik dalam aplikasi sebenar dan juga pada skala besar.

**HETEROGENEOUS FENTON DEGRADATION OF OFLOXACIN IN
AQUEOUS SOLUTION USING Fe₃O₄-ZEOLITE, Fe₃O₄-
MONTMORILLONITE AND Fe₃O₄-MONTMORILLONITE ALGINATE
COMPOSITES**

ABSTRACT

The primary aim of this study is to develop an economical, stable and effective heterogeneous catalyst for wastewater remediation via the Fenton oxidation process. Fe₃O₄ can effectively activate H₂O₂ to produce hydroxyl radicals, but the particles agglomerate easily. To solve this problem, Fe₃O₄-zeolite (FeZ) and Fe₃O₄-montmorillonite (FeM) composites were synthesized via a facile co-precipitation method and characterized using various techniques. The performance of each of the catalysts was evaluated via the Fenton degradation of ofloxacin (OFL), an antibiotic and a recalcitrant pollutant because of its high activity and poor biodegradability. The effect of parameters such as amount of Fe precursor, catalyst dosage, initial solution pH, initial OFL concentration, different oxidants, H₂O₂ dosage, reaction temperature and inorganic salts on the OFL removal percentage were investigated. Loading of Fe₃O₄ onto zeolites resulted in the formation composites with higher surface area and pore volume. Experimental results revealed that as much as 88% OFL from the aqueous OFL solution 20 mg/L and 51.2% total organic carbon (TOC) could be removed in 120 min using FeZ-8 catalyst at the optimum condition. Since montmorillonite is capable to adsorb OFL at higher concentration, the OFL initial concentration was adjusted to 50 mg/L for FeM. The efficiency of the FeM composite in the removal of OFL from the aqueous solution was also investigated using the same experimental parameters. Under the optimum condition and at the pH of the neutral

OFL solution via the heterogeneous Fenton in the presence of H_2O_2 was almost 81%, while the total organic carbon (TOC) reduction was about 56% in 120 minutes. Both FeZ and FeM composites show a decrease in the removal percentage by as much as 8.89 and 21.42% in the fifth cycle, respectively and this was assumed to be due to the high leaching of the Fe ions which are 56.19 and 65.37%, respectively. Since the Fenton degradation efficiency of FeM is higher compared to FeZ, the FeM composite was immobilized into calcium alginate to form FeMA composite beads to overcome this problem. Under otherwise the same condition, the OFL removal percentage using FeMA beads reaches about 80%, while the total organic carbon (TOC) removal reaches about 53% with a minimal decrease (2%) in the removal percentage in the fifth cycle. The composite beads could be easily separated, recycled and the leaching of iron ions is low, 0.142 mg/L (at the fifth cycle). Based on the experimental results, it is thus concluded that the FeMA composite beads synthesized has a great potential as a heterogeneous Fenton catalyst for the degradation of organic pollutants such as antibiotic in real and large scale applications.

CHAPTER 1

INTRODUCTION

1.1 Background

Water is a very precious resource and an essential requirement in the sustenance of all forms of life (Yeleliere et al., 2018). Unfortunately, water pollution has reached an alarming state due to various activities as shown in Figure 1.1 (Kaus et al., 2021). For instance, a very frequently prescribed antibiotic, ofloxacin (OFL) has been detected in hospital effluent, surface water and wastewater treatment plants (Rytwo and Zelkind, 2021; Vaizoğullar, 2020). The presence of OFL contaminates the environment and could lead to the development of antibiotic resistant microbes, and thus should be treated properly (Vaizoğullar, 2020).

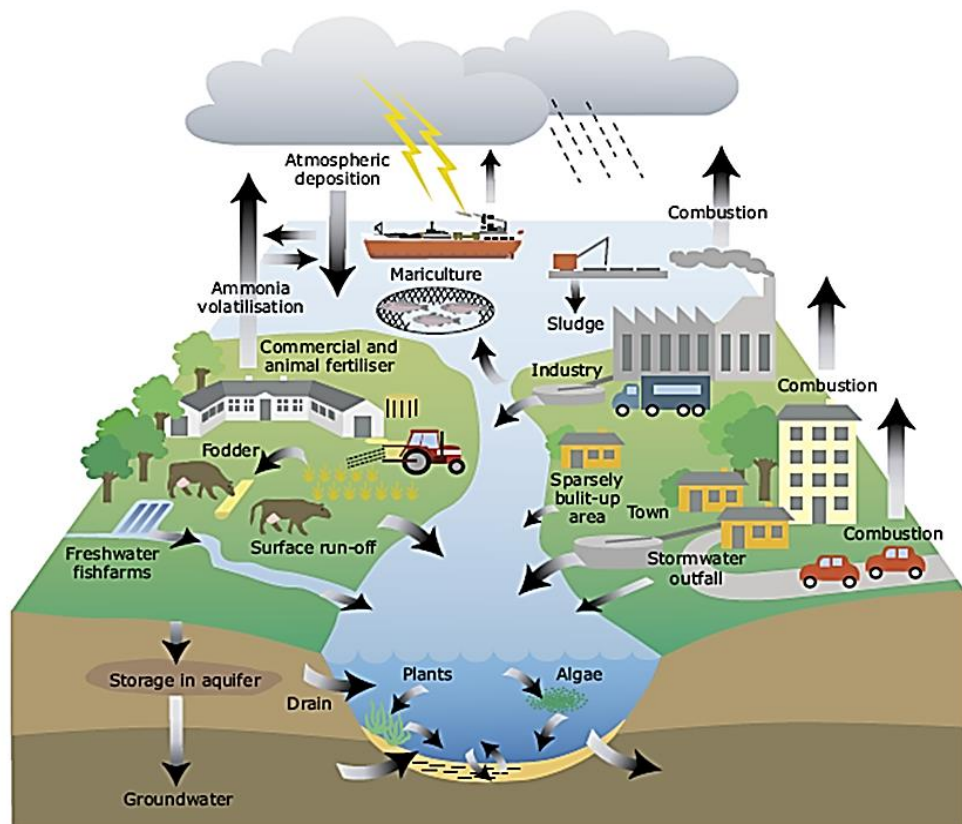


Figure 1.1: Sources of water pollution.

Different treatment techniques, including physical, chemical, and biological technologies, are currently being employed in the water purification process (Crini and Lichtfouse, 2019). However, the methods used by most wastewater treatment plants (WWTPs) have limited capacity for the thorough elimination of pharmaceuticals and personal care products (PPCPs) from wastewater, as they were not initially designed for removing PPCPs (Dong et al., 2016). Furthermore, specific physical and biological methods that are also being employed have some limitations. For instance, most physical treatment methods only transfer the pollutants to another phase rather than destroying them (Dong et al., 2016). Likewise, the biological treatment method could lead to the development of antibiotic-resistant bacteria (Zhang, 2016).

Unlike the physical and biological treatment methods, chemical oxidation methods such as homogeneous and heterogeneous Fenton treatment methods can mineralize a wide range of organic pollutants (Varjani and Sudha, 2018). The Fenton reaction is an effective process that has gained widespread acceptance due to its efficiency in degrading and even mineralizing persistent organic contaminants by using the highly reactive hydroxyl radicals ($\bullet\text{OH}$) generated from H_2O_2 using Fe^{2+} from a Fenton reagent (Tian et al., 2020b). The process is cheap, promising and environmentally benign (Herney-Ramirez et al., 2010; Nguyen et al., 2011). However, compared to the homogeneous Fenton process, the easy recovery of the catalyst after application in the heterogeneous Fenton process makes it more convenient. Various heterogeneous Fenton catalysts, including Fe_3O_4 nanoparticles (Xu and Wang, 2012), Fe-Mn oxide (Li et al., 2019a), and Cu-Fe oxide (Cheng et al., 2019), have been proposed.

Fe_3O_4 nanoparticles have received significant attention among the catalysts due to their low toxicity and biocompatibility properties (He and Gao, 2010). Moreover, another potential heterogeneous catalyst that has gained attention involved the immobilization of Fe_3O_4 on inorganic or organic solid supports (Hu et al., 2011). Such supports, including activated carbon (Jaafarzadeh et al., 2015), carbon nanotubes (Cleveland et al., 2014), graphite oxide (Hua et al., 2014), SBA-15 (Mazilu et al., 2017) etc., are capable of improving the efficiency of the Fenton process. Notwithstanding, there's still the need for efficient and cheaper alternative post-treatment process to recover the particles for regeneration and subsequent re-use which is important from economical point of view. The immobilization of the catalysts onto polymers including chitosan (Aoudjit et al., 2021), alginate (Sarkar et al., 2015) etc. have been reported to minimize catalyst loss, reduce aggregation, improve the stability of the catalyst, enhance reusability and also ease the catalyst recovery process after application (Balakrishnan et al., 2020).

1.2 Problem Statements

For the past few years, the high consumption of antibiotics has resulted in their detection (Figure 1.2) in surface, ground, drinking, and wastewater worldwide (Chen et al., 2019). Their presence threatens the ecological environment due to their high activity, stability and slow biodegradation since antibiotics are harmful to microorganisms (Wang et al., 2019e; Zhu et al., 2020).

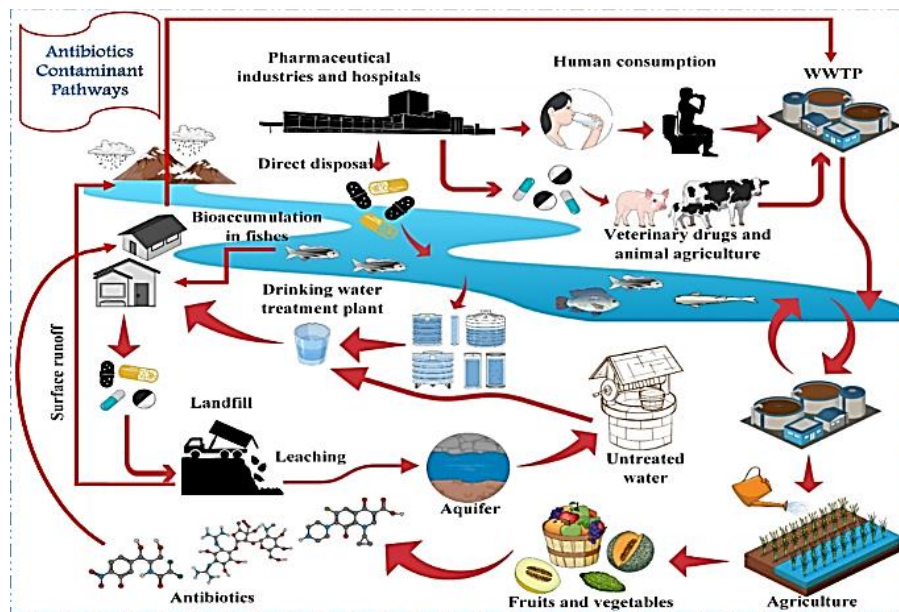


Figure 1.2: Pathways of antibiotics in different environmental matrices (Bhagat et al., 2020).

Among the antibiotics, ofloxacin (OFL) is an extensively used 2nd-generation fluoroquinolone antibiotic due to its good antibacterial activity (Liu et al., 2019b; Zhao et al., 2020). However, approximately 90% of the antibiotics are excreted via urination in their original form 48 h after administration (Kaur et al., 2019). The presence of OFL in water results in unpleasant odours and may also present a significant risk to aquatic species due to its toxicity (Lin and Lin, 2019; Wuana et al., 2015a). The detection of antibiotics such as OFL in wastewater treatment plants has been reported by various researchers, thus indicating the inefficiencies of the conventional treatment methods (Changotra et al., 2019). Therefore, developing a more effective way to remove an antibiotic such as OFL from wastewater becomes imperative.

Homogeneous or heterogeneous Fenton reactions are well-known advanced oxidation processes (AOPs). They have been reported to be very highly potential methods for treating wastewater containing various non-biodegradable organic

pollutants. However, their overall potential and large scale application are restricted due to several disadvantages (Caudo et al., 2006; Tarr, 2003), which are:

- (i) The reaction generates iron hydroxide sludge which demand secondary steps to meet environmental standards and regulations;
- (ii) The reaction usually requires very tight working pH (pH 2–3); and
- (iii) The deactivation of iron ions in the presence of complexation agents such as phosphate anions and intermediates from the oxidation products.

Compared to the homogeneous Fenton process, the insoluble catalysts and their easy recovery after application in the heterogeneous Fenton process makes it more convenient and a better choice (Gou et al., 2021). Among the heterogeneous catalysts, Fe_3O_4 magnetic nanoparticles are more active in terms of hydroxyl radicals production via the Fenton-like processes (Bai et al., 2017). Sequel to that, many researchers have reported various methods of enhancing the efficiency of the heterogeneous Fenton process. The common method involves immobilization of the catalyst onto various supports. Notwithstanding, most of the reported supports used are only commercially available. A cheaper alternative would be clay. Clay minerals are naturally available, abundant, cost-effective, and environmentally benign (Han et al., 2019; Herney-Ramirez et al., 2010). In addition to that, clay has high surface area, high pore volume, high sorption properties, and ion exchange potential (Uddin et al., 2019; Vinati et al., 2015). These properties imply that clay minerals e.g. montmorillonite are good candidates that could be used to support Fe_3O_4 . Apart from clay, zeolites are also porous and high surface area materials which are frequently been used as conventional adsorbents, and could also serve as a support for immobilization of Fe_3O_4 (Zhang et al., 2015). Thus, in this work Fe_3O_4 -zeolite and Fe_3O_4 -motmorillonite composites will

be produced via a facile process for the activation of H_2O_2 to produce $\bullet\text{OH}$ radicals in the degradation of OFL via Fenton process.

On the other hand, the phase separation problem encountered during the recovery process after the catalytic reaction is also a significant challenge and could limit the application of catalyst at industrial level. The encapsulation of the powdered catalyst into a polymer matrix such as calcium alginate could address such limitations.

1.3 Objectives of the Proposed Study

1. To synthesize Fe_3O_4 -zeolite and Fe_3O_4 -montmorillonite composites, using facile co-precipitation process, and immobilize the best performing composite into calcium alginate beads.
2. To characterize the structural and physicochemical properties of the composites using various methods.
3. To determine the optimum parameters and the efficiency of Fe_3O_4 -zeolite, Fe_3O_4 -montmorillonite and immobilized composites, towards removing ofloxacin (OFL) from an aqueous solution, and conduct reusability studies.
4. To study the kinetics for the removal of OFL from aqueous solution using Fe_3O_4 -zeolite, Fe_3O_4 -montmorillonite and Fe_3O_4 -montmorillonite alginate composites, and correlate the catalytic activity of the composites with their physicochemical properties.

1.4 Scope of Study

The scope of the present study involves the synthesis of Fe₃O₄-zeolite and Fe₃O₄-clay-based composites, their characterization, and their application as heterogeneous Fenton catalysts for the degradation of OFL in an aqueous solution. The heterogeneous Fenton catalysts include Fe₃O₄-zeolite composite, Fe₃O₄-montmorillonite composite, and the immobilization of Fe₃O₄-montmorillonite composite into calcium alginate (CA) beads. The study is limited to Fe₃O₄-zeolite and Fe₃O₄-montmorillonite composites produced via a facile co-precipitation and characterized using various characterization techniques. The catalyst will be activated using H₂O₂ for the Fenton degradation of ofloxacin in aqueous solution. The best performing composite among Fe₃O₄-zeolite and Fe₃O₄-montmorillonite will be selected and loaded into calcium-alginate beads.

1.5 Hypothesis and Significance of the Study

The hypothesis this thesis can be summarized as follows:

1. The formation of Fe₃O₄ composites will prevent Fe₃O₄ agglomeration and the immobilization will improve their catalytic activity and enhance the degradation of OFL from aqueous solution.
2. The immobilization of Fe₃O₄ onto zeolite, montmorillonite and with alginate will ease the recovery of the catalyst and reduce the leaching of Fe₃O₄ into the aqueous solution.
3. The immobilization of Fe₃O₄ onto zeolite, montmorillonite and with alginate will allow the Fenton reaction to take place in greater pH range and not limited to only the pH 2-3 environment.

The significance of this study is because OFL is the common antibiotic detected in treated wastewater and wastewater plants. This signifies the fact that the current treatment methods are not sufficient to treat the polluted water. It is known that the presence of antibiotic in water have many negative effects to the environment including to the microorganism. Therefore, finding a better solution to treat water contaminated with antibiotic is important.

1.6 Thesis Outline

This thesis has been divided into 7 chapters. The first chapter presents an overview of the work, including the problem statements, research objectives, and thesis scope. The second chapter provides a literature review of the topic. The methodology of the work, including chemicals used during synthesis and heterogenous Fenton degradation studies, in addition to the instruments employed for the characterizations, are elaborated in the third chapter. In Chapters Four, Five, and Six, findings on the characterizations and the application of Fe_3O_4 -zeolite composite, Fe_3O_4 -montmorillonite composite, and Fe_3O_4 -montmorillonite composite/CA beads as heterogeneous Fenton catalysts for the degradation of OFL in aqueous solution are discussed. Finally, Chapter seven concludes the research's major findings and lists recommendations for future work in this field.

CHAPTER 2

LITERATURE REVIEW

2.1 Background

In the present 21st century, water pollution has remained one of the leading global environmental challenges, following the discharge of toxic substances from various anthropogenic activities (Reddy, 2017). Among the toxic substances being discharged, a group of contaminants, including pharmaceuticals and personal care products (PPCPs), contrast media, plasticizers, nanomaterials, flame retardants, surfactants, food additives, wood preservatives, pesticides, hormones etc., has been recognized as significant water pollutants and are termed as *emerging contaminants* (ECs), (Lima, 2018; Rodriguez-Narvaez et al., 2017). Figure 2.1 summarizes the emerging contaminants found in water bodies and the challenges in treating these EC compounds. However, the environmental fate of ECs and their behavior is still largely unknown (Sarkar et al., 2019).

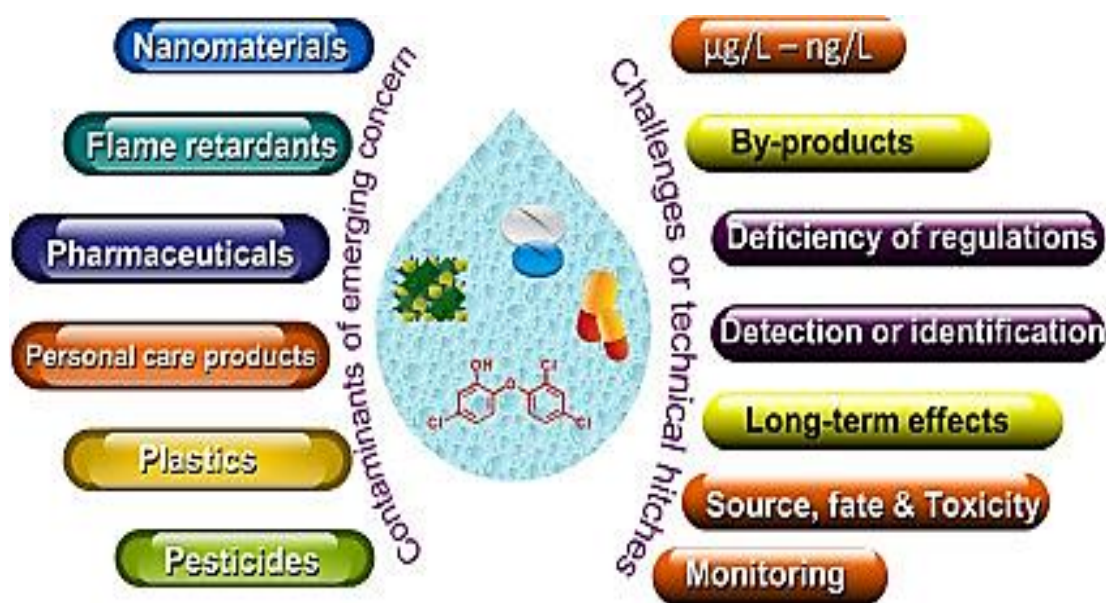


Figure 2.1: Contaminants of emerging concern and existing challenges in their treatment (Reddy, 2017).

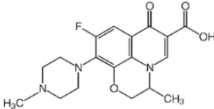
As a class of ECs, PPCPs are also components with a high concentration in wastewater, amongst which antibiotics have received significant attention (Corada-Fernández et al., 2017; Li et al., 2018). Antibiotics are chemotherapeutic agents used to inhibit the growth and eradicating bacterial infections (Calvete et al., 2019). Unfortunately, during production and wide used applications including in farming, a large amount of antibiotics are released back into the environment through urine and faeces, resulting in a serious pollution (Wang and Zhuan, 2020). Among the antibiotics, fluoroquinolones, including ofloxacin, are frequently detected in wastewaters and surface waters (Chen et al., 2015; He et al., 2015). It is also reported that the techniques currently employed by most wastewater treatment plants (WWTPs) have limited capacity for the thorough elimination of PPCPs, including OFL from wastewater (Dong et al., 2016).

2.2 Ofloxacin

Ofloxacin (OFL, Table 2.1) is a second-generation fluoroquinolone antibiotic with the chemical formula of $C_{18}H_{20}FN_3O_4$ and chemical name 9-fluoro-2,3-dihydro-3-methyl-10-(4-methyl-1-piperazynyl)-7-oxo-7H-pyrido-[1,2,3-de]-1,4-benzoxazine-6-carboxylic acid (Sharma et al., 2011; Wang et al., 2019d). It was patented in 1980 and subsequently approved for medical use in 1985 (Janos and Robin, 2006; Sun et al., 2012a). Currently, OFL is frequently prescribed for the treatment of bronchitis, infectious diarrhoea, pneumonia, chlamydia, pelvic inflammatory disease, eye infections, digestive infections, ear infections, gonorrhoea, respiratory tract infections, urinary tract infections, gastrointestinal infections, and skin infections (Chen et al., 2013; Kaur et al., 2019; Mushtaq et al., 2020).

However, due to its partial metabolism in the body after ingestion, biological resistance, and the large volume of pharmaceutical wastewater which is being released untreated, studies have reported the detection of OFL with different concentrations in hospital wastewater (25,000 – 35,000 ng/L), municipal wastewater treatment plants (53 – 1800 ng/L) and surface water (10 – 535 ng/L), with residence time of about 10.6 days (Enick and Moore, 2007; Esposito et al., 2017; Peres et al., 2015).

Table 2.1: Molecular structure and some physicochemical properties of OFL

Property		Reference
Chemical formula	C ₁₈ H ₂₀ FN ₃ O ₄	(Wang et al., 2015a)
CAS number	82419-36-1	(Wang et al., 2019a)
Therapeutic group	Antibiotic	(Michael et al., 2010)
Chemical structure		(El Bekkali et al., 2017)
Molecular weight (g/mol)	361.4	(Kong et al., 2017)
Color	White	(Onyenze and Edozie, 2021)
Melting point	270 – 273 °C	(Michael et al., 2010)
Solubility in water at 25 °C (mg/mL)	60 (pH = 2 – 5); 4 (pH = 7); 303 (pH = 9.8)	(Hapeshi et al., 2010)
Partition coefficient	-0.39	(Wang et al., 2019a)
Dissociation constant	6.10/8.28	(Wang et al., 2019a)
Octanol/water partition coefficient log k_{o/w}	0.41 (pH 7); 0.33 (pH 7.2); 0.28 (pH 7.3)	(Michael et al., 2010)
Isoelectric constants	pK _{a1} = 5.98; pK _{a2} = 8.00	(Gao et al., 2019)
Vapour pressure (mm Hg)	1.55E-0.13	(Michael et al., 2010)
Henry constant at 25 °C (atm/m³ mole)	4.98E-0.20	(Michael et al., 2010)
Pharmacokinetic parameters	Bioavailability (%) = 70 – 90 Time of half-life (h) = 5 – 7.4 Excretion in urine (%) = 80	(Michael et al., 2010)

The presence of OFL in water results in high colour with unpleasant odours (Sun et al., 2012b; Wuana et al., 2015b). It may also lead to microbial resistance among pathogens or the death of microorganisms effective in wastewater remediation (Peres et al., 2015; Su et al., 2022; Wuana et al., 2015b). Thus, identifying the proper processes for the thorough and complete elimination of OFL from wastewater is essential.

Nowadays, the well-known methods commonly employed to remove persistent organic contaminants, including OFL, are the Advanced Oxidation Processes (AOPs). These processes involve generating highly reactive and non-selective free radical species, which can destroy many organic pollutants. The AOPs are currently categorized as environmentally friendly processes since they neither result in secondary pollution nor the generation of excessive hazardous sludge (Leonel et al., 2021; Mishra et al., 2017; Varnagiris et al., 2020). Various AOPs including photocatalytic degradation (Zhang et al., 2020a), heterogeneous photo-Fenton (Du et al., 2020), heat-activated persulfate oxidative degradation (Li et al., 2022), photoelectrocatalytic degradation (Li et al., 2014), ozonation (Xu et al., 2021), heterogeneous Fenton degradation (Qin et al., 2021b) etc. have been studied for degradation of OFL. Although, the heterogeneous Fenton process involves the use of certain catalysts for the activation of H_2O_2 to produce $\bullet OH$, some of these processes require heat and/or light to be effective. Presently, many studies regarding the degradation of OFL via AOPs such as photocatalytic degradation process have been reported. However, researches involving the degradation of OFL via Fenton process are still scarce and deserves to be explored.

2.3 Wastewater Treatment Methods

Wastewater treatment methods are highly diversified and classified into three broad methods which are physical, chemical, and biological methods (Sum, 2004). Wastewater treatment methods such precipitation, oxidation, flotation, evaporation, carbon adsorption, phytoremediation, solvent extraction, membrane filtration, electrochemistry, ion exchange, or biodegradation, are currently being used but with certain limitations, as summarised in Table 2.2 (Crini and Lichtfouse, 2019). Choosing the most sustainable wastewater treatment technology among all the possible options is a difficult task, as economic, environmental and social factors must all be considered (Arroyo and Molinos-Senante, 2018).

Table 2.2: Different wastewater treatment methods and their advantages and limitations.

Method	Feature	Advantages	Limitation	References
Coagulation /Flocculation	Pollutant's uptake and separation of the products formed.	<ul style="list-style-type: none"> • Varieties of chemicals are available commercially. • Cheap • Good sludge settling and dewatering characteristics. • Significant reduction in the biochemical oxygen demand and chemical oxygen demand. • Capability to inactivate bacteria. • Efficient and rapid for insoluble contaminants (pigments, etc.) removal. 	<ul style="list-style-type: none"> • Poor arsenic removal. • High sludge generation. 	(Bratby, 2016)
Chemical precipitation	Pollutant's uptake and separation of the products formed.	<ul style="list-style-type: none"> • Applicable to a variety of metals. • Efficient and economically feasible. 	<ul style="list-style-type: none"> • Consumes chemicals e.g., H₂S, Oxidants etc. • Poor performance in removing low concentration of metals. 	(Henze et al., 1997)

Table 2.2. Continued

Method	Feature	Advantages	Limitation	References
Flotation	Separation process.	<ul style="list-style-type: none"> • Capable of removing small and low-density particles. • Retention time is low. • Applicable as efficient tertiary treatment in the paper and pulp industry. 	<ul style="list-style-type: none"> • Expensive. • pH-dependent selectivity. 	(Sharma and Sanghi, 2012)
Biological method	Use of biological cultures.	<ul style="list-style-type: none"> • Facile, acceptable and economically feasible. • Significant biochemical oxygen demand removal. • Color attenuation is appreciable. 	<ul style="list-style-type: none"> • The process is slow. • Poor biodegradability towards certain molecules. • Requires optimally favourable environment. 	(Henze et al., 1997); Rathoure (2015)
Adsorption	Use of solid material.	<ul style="list-style-type: none"> • Facile, effective and cheap. • Various adsorbents are commercially available. • Applicable to a wide range of pollutants. 	<ul style="list-style-type: none"> • Clogging and rapid saturation of reactors. • pH-sensitive performance. • Matrix could degrade under certain conditions. 	Mohan and Pittman Jr (2007)
Advanced oxidation processes (AOPs)	Chemical process that employ oxidizing agent or ozone and/or light.	<ul style="list-style-type: none"> • Production of reactive radicals via an in-situ process. • Zero sludge generation. • Rapid process. • Mineralization capability. • Applicable for both organic and inorganic pollutants. 	<ul style="list-style-type: none"> • By-product's formation. • Various technical constraints and as energy intensive conditions. • The process is pH-dependent. 	Parsons (2004)

The Advanced Oxidation Processes (AOPs) which are classified based on the available physico-chemical processes (Figure 2.2) have continued to attract significant attention from researchers due to their unique features, non-selective destruction of organic pollutants and high performance (Niu et al., 2020).

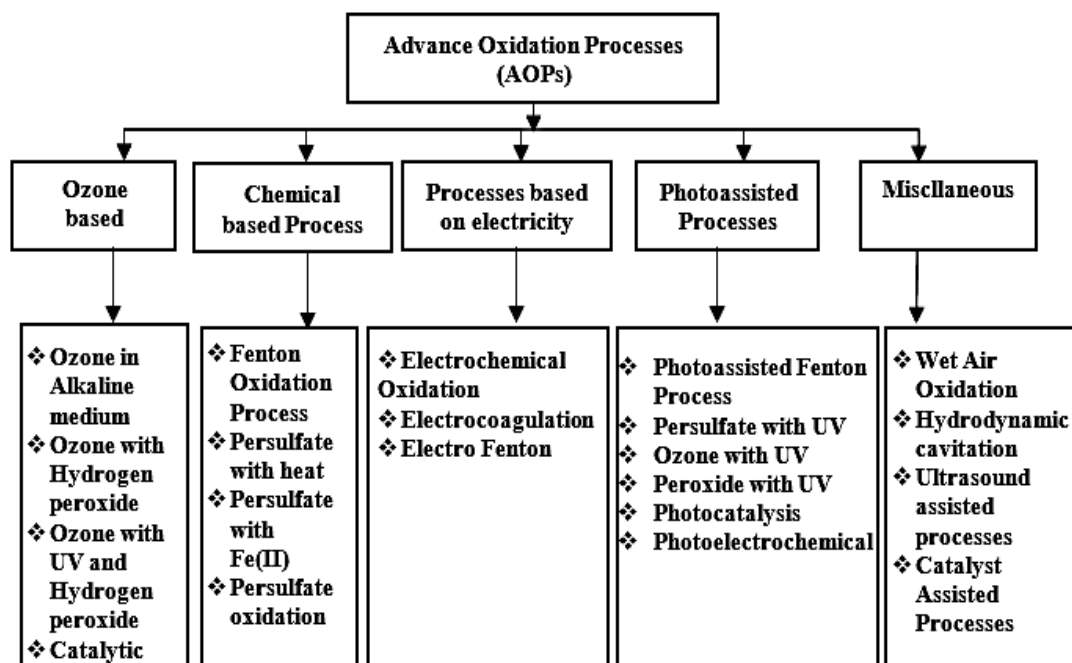


Figure 2.2: Summary of the different advanced oxidation processes (Gautam et al., 2019).

AOPs involves generation of highly reactive free radicals, mostly hydroxyl radicals ($\bullet\text{OH}$). Such hydroxyl radicals are strong oxidizing agents which behave as electrophiles and are therefore capable of attacking and degrading many organic nucleophiles, with CO_2 being reported as the most stable end-product of the processes (Stasinakis, 2008). The AOPs are also classified based on the mechanism involved in the generation of transient hydroxyl radicals.

2.3.1 Fenton Process

The Fenton process (Figure 2.3) is one of the AOPs discovered and first reported by the French scientist H.J.H Fenton in 1894 (Tian et al., 2020c). The process has gained widespread acceptance due to its efficiency in degrading and even mineralizing persistent organic contaminants using the highly reactive hydroxyl radicals ($\bullet\text{OH}$) generated from H_2O_2 using Fe^{2+} from a Fenton reagent (Tian et al., 2020b). Generally, the mechanism of the Fenton process could be broadly described by Equations 2.1 to 2.2 below, which are (i) production of hydroxyl radicals with simultaneous oxidation of iron and followed by (ii) the reduction of Fe^{3+} back to Fe^{2+} and the cycle continue (Giannakis, 2019):

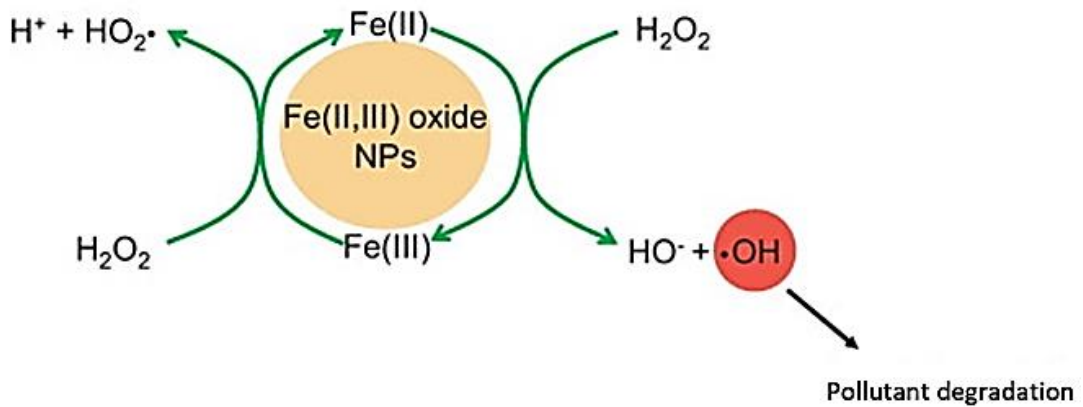
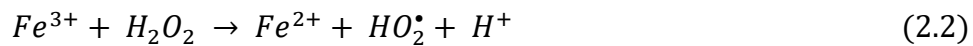
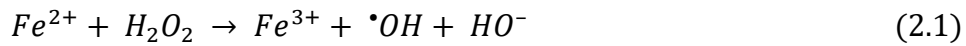


Figure 2.3: Heterogeneous Fenton degradation (Rusevova et al., 2012).

The Fenton process has variants, and the classification is shown in Figure 2.4. The process can be divided into two, based on the usage of external energy. The external energy, including light, ultrasound, and electricity, further enhances the degradation efficiency. The two processes involving energy use are the extended and

hybrid Fenton Processes. On the other hand, the conventional Fenton process does not involve the use of external energy.

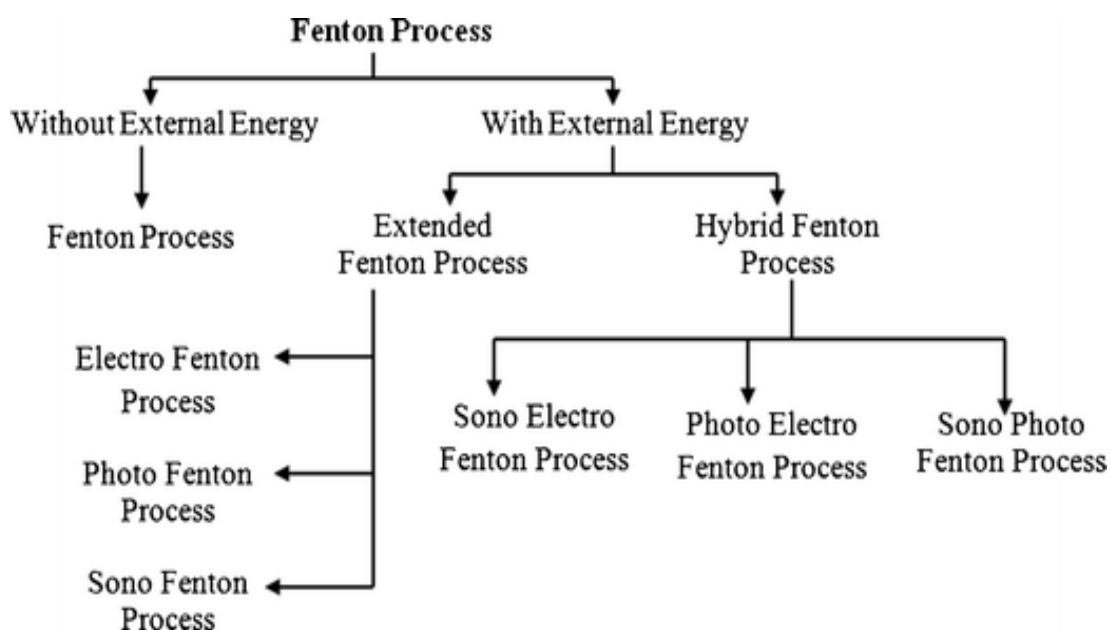


Figure 2.4: Classification of Fenton process (Nidheesh et al., 2013).

The conventional Fenton process, which can either be heterogeneous or homogeneous, has a short reaction time, does not require complicated apparatus and is cost-effective since no energy input is needed in activating H_2O_2 . The homogeneous Fenton process usually involves the use of soluble form of iron (Fe^{2+}) to catalyse hydroxyl radicals formation (Khataee et al., 2015). However, to overcome the shortcomings of the homogeneous Fenton process such as, formation of ferric hydroxide precipitate at higher pH and impracticable catalyst separation (Pouran et al., 2018), various heterogeneous Fenton catalysts, including Fe_3O_4 nanoparticles (Xu and Wang, 2012), Fe-Mn oxide (Li et al., 2019a), and Cu-Fe oxide (Cheng et al., 2019), have been proposed. Fe_3O_4 nanoparticles have received significant attention among the catalysts due to their low toxicity and biocompatibility properties (He and Gao, 2010). Moreover, another potential heterogeneous catalyst that has gained attention involved the immobilization of Fe_3O_4 on inorganic or organic solid supports (Hu et al.,

2011). Supports including activated carbon (Jaafarzadeh et al., 2015), carbon nanotubes (Cleveland et al., 2014), graphite oxide (Hua et al., 2014), SBA-15 (Mazilu et al., 2017), etc. are capable of improving the efficiency of the Fenton process and also eased the catalyst recovery process after application. However, they are only commercially available. Thus, the choice of an appropriate support is critical (Zhang et al., 2019b). Therefore, emphasis is placed on candidates that are cheap, available for wide pH range, have high catalytic activity and stability. Going by the above requirements, clay and clay-like minerals such as zeolites, halloysites, montmorillonite, bentonites etc. can be promisingly applied for this purpose. This is because clay and clay-like materials are naturally available and abundant, cost-effective, and environmentally benign (Herney-Ramirez et al., 2010; Lazaratou et al., 2020). The efficiencies recorded using the heterogeneous Fenton process have been reported in literatures.

For instance, Guo et al. (2014) reported the degradation of rhodamine B dye via a heterogeneous photo-Fenton process, using Fe_2O_3 -kaolin as heterogeneous photocatalyst. Before incorporating Fe_2O_3 , the specific surface area of kaolin was $19.47 \text{ m}^2/\text{g}$. However, the introduction of Fe_2O_3 increased the surface area of the composites to $39.32 \text{ m}^2/\text{g}$. Unlike the homogeneous photo-Fenton process, which is possible within a limited pH range, the composites were effective within pH range of 2.21 – 10.13. As much as 98% discoloration and 66% mineralization were achieved within 120 mins at optimal conditions. Such results made the composites promising.

Apart from kaolin, Chen et al. (2009) tested iron-pillared montmorillonite as a heterogeneous catalyst for the photo-Fenton degradation of reactive brilliant orange X-GN under visible light. In their case, 98.6 % discoloration and 52.9% TOC removal were achieved within 140 mins. This provides another inspiration for the high-

performance expectation of iron-supported clay minerals in the heterogeneous photo-Fenton process.

In another study involving montmorillonite, De León et al. (2017) reported that introducing iron into montmorillonite gave composites a higher surface area than pure clay. Likewise, the composites showed enhanced performance in terms of application, and low leaching was observed. This indicates that the catalysts could retain the iron incorporated during their preparation.

Apart from montmorillonite, other clays, including expanded perlite, have been used to support iron in preparing composites for their subsequent use as heterogeneous catalyst in Fenton photodegradation process. For instance, Jiang et al. (2017) synthesized Fe₂O₃/expanded perlite composites via the hydrothermal method and used them to degrade rhodamine B and metronidazole in the presence of H₂O₂ under visible light. The catalysts remained efficient over a pH range of 2 – 10. The degradation of rhodamine B dye reached 99% within 90 mins, with low iron leaching, and the Fenton catalyst remained stable even after five cycles.

Also, Liang et al. (2015) coated Fe₂O₃ nanoparticles onto diatomite for use as heterogeneous catalysts for the photo-Fenton degradation of rhodamine B dye. Decolorization efficiency of 99.14% and TOC removal of 73.41% were recorded for rhodamine B. The authors believed the high efficiencies due to the adsorption's synergetic effects by diatomite and the hydroxyl radicals produced by heterogeneous photo-Fenton reactions. Fortunately, the decolorization efficiency was still higher than 90% even after 5 cycles.

Besides iron, Chanderia et al. (2017) studied the photo-Fenton degradation of sunset yellow FCF using copper-loaded bentonite (prepared by wet impregnation method) and hydrogen peroxide. The degradation of sunset yellow dye was appreciable and had a degradation rate of 1.55×10^4 per second.

A number of authors have reported, apart from monometallic catalysts (Shi et al., 2021; Zhang et al., 2020b). For instance, D-Fe@sepiolite (monometallic) and D-FeCu@sepiolite (bimetallic) were prepared by loading Fe and Fe-Cu bimetal of 1D sepiolite and used by Tian et al. (2020c) for the Fenton degradation of OFL. The pollutant was almost completely degraded at 120 min over D-FeCu@sepiolite in the presence of H_2O_2 , while the efficiency in the presence of D-Fe@sepiolite was only around 70%.

Table 2.3 below summarizes the efficiencies recorded during the treatment of wastewater contaminated by OFL using various Fenton processes. In general, it can be concluded that the photo-Fenton processes have been shown to have better efficiencies and complete or near complete degradation of the antibiotic compared to the conventional Fenton processes. This indicate that the reaction can be further enhanced in the presence of light. Metals such as Cu and Mn have been shown to be another good alternative for Fenton catalysts. The binary metal oxides of Cu- or Mn- with Fe_3O_4 have also been reported to show excellent Fenton reaction activity.

Table 2.3: Efficiencies during the treatment of OFL polluted water via Fenton process.

No	Catalyst	Types of Fenton reaction	Condition	Efficiency/rate constant	References
1	FeSO ₄ .7H ₂ O	photo-Fenton	[OFL] = 10 mg/L Dosage = 5 mg/L pH = 3 Time = 90 min [H ₂ O ₂] = 2.714 mmol/L	100 %	(Michael et al., 2010)
2	Fe ₃ O ₄ @FeOOH	Fenton	[OFL] = 10 mg/L Dosage = 25 mg/L pH = 6.5 Time = 60 min [H ₂ O ₂] = 9.7 mol/L	64 %	(Jin et al., 2017b)
3	Cu-MIO	Fenton	[OFL] = 12 mg/L Dosage = 25 mg/L pH = 6.4 [H ₂ O ₂] = 9.7 mmol/L	0.0405/min	(Tian et al., 2017)
4	Silicon based catalyst (Fe@MPSi)	Fenton	[OFL] = 30 mg/L Dosage = 1 g/L Time = 2 hrs [H ₂ O ₂] = 2000 mg/L	18 %	(Zheng et al., 2017)

Table 2.3. Continued

No	Catalyst	Types of Fenton reaction	Condition	Efficiency/rate constant	References
5	Cu-Alg	Fenton	[OFL] = 20 mg/L Dosage = 1 g/L Time = 120 min pH = 3 [H ₂ O ₂] = 40 mmol/L	36%	(Titouhi and Belgaied, 2016)
6	Fe ₃ O ₄ -AC	Fenton	[OFL] = 12 mg/L Dosage = 0.5 g/L Time = 5 min pH = 3.3 [H ₂ O ₂] = 20 mM	56.5%	(Liu et al., 2019b)
7	FeCp@sepiolite	Photo-Fenton	[OFL] = 10 mg/L Dosage = 50 mg Time = 150 min pH = 3 [H ₂ O ₂] = 2.0 mmol/L	100%	(Tian et al., 2018)
8	Sludge derived carbon (SC)	Fenton	[OFL] = 30 mg/L Dosage = 1 g/L Time = 540 min [H ₂ O ₂] = 2.0 mmol/L	91.5%	(Yu et al., 2019)

Table 2.3. Continued

No	Catalyst	Types of Fenton reaction	Condition	Efficiency/rate constant	References
9	Fe(II)	Fenton	[OFL] = 24.93 mmol/L [Fe(II)] = 0.003 mmol/L Time = 120 min pH = 4 [H ₂ O ₂] = 1.5 mmol/L	99.5%	(Pi et al., 2014)
10	Fe-Dis@Sep	Photo-Fenton	[OFL] = 10 mg/L Dosage = 0.5 g/L Time = 150 min pH = 3 [H ₂ O ₂] = 2.0 mmol/L	92.9%	(Tian et al., 2020a)
11	Biogenic Fe-Mn oxides (bio-FeMnO _x)	Photo-Fenton	[OFL] = 30 mg/L Dosage = 5 mg/L Time = 2 h [H ₂ O ₂] = 4.1 μM	98.1%	(Du et al., 2020)
12	Fe ₃ O ₄ @S-doped ZnO	Fenton	[OFL] = 10 mg/L Dosage = 0.25 g/L Time = 120 min pH = 6.5 [H ₂ O ₂] = 5.0 mL/L	100%	(Wang et al., 2020)